

BPM-Net: non-contact blood pressure measuring network based on face videos

Jialiang Zhuang^a, Bin Li^b, Yun Zhang^c, Xiujuan Zheng^{a,*}

^aCollege of Electrical Engineering, Sichuan University, Chengdu, Sichuan, China

^bSchool of Computer Science, Northwest University, Xi'an, China

^cSchool of Information Science and Technology, Xi'an Jiaotong University, Xi'an, China

Abstract

Blood pressure indicates cardiac function and peripheral vascular resistance and is critical for disease diagnosis. Traditionally, blood pressure data are mainly acquired through contact sensors, which require high maintenance and may be inconvenient and unfriendly to some people (e.g., burn patients). In this paper, we proposed an efficient non-contact blood pressure measurement network based on face videos. First, an innovative oversampling training strategy is proposed to handle the unbalanced data distribution. The input video sequences are first normalized and converted to our proposed YUVT color space. Then the spatio-temporal slicer encodes it into a multi-domain spatio-temporal mapping. Finally, the feature extractor composed of a series backbone network and LSTM fits the high-dimensional feature, which is fed into blood pressure classifier to locate the blood pressure interval. The blood pressure calculator combines the results of the feature extractor and the blood pressure classifier to output the final blood pressure value. We tested BPM-Net on MMSE-HR dataset, the MAE of systolic blood pressure reached 12.35 mmHg and that of diastolic blood pressure reached 9.5 mmHg. Experimental results on MMSE-HR show that the network outperforms existing state-of-the-art methods.

Keywords: non-contact, blood pressure measurement, oversampling training strategy, face video

*Corresponding author xiujuanzheng@scu.edu.cn

1. Introduction

Blood pressure is a primary physiological parameter of the human body and an essential basis for disease diagnosis. Cardiovascular diseases are the leading cause of death globally. Most of them are highly related with hypertension. In this context, convenient ordinary monitoring of blood pressure in daily life becomes critical.

Many outstanding scientists [1, 2] have devoted themselves to the study of calculating blood pressure by extracting the waveform shape characteristics of the single point pulse wave and obtained good results, which means that single point pulse wave can effectively reflect the change characteristics of blood flow in the human cardiovascular system in different heart cycles. However, they all need the blood volume pulse (BVP) obtained by special sensors, which greatly limits the application range of blood pressure calculation. Now there are many excellent works that can accurately simulate BVP based on face video and accurately calculate heart rate and heart rate variability. Some works such as RthymNet [3] showed that spatio-temporal map of face videos can perfectly simulate BVP and blood flow state in blood vessels, Cheng [4] also proposed a method to convert BVP into pressure pulse wave, which proves that there is an essential relationship between single-point BVP and pressure pulse wave. These results of the previous results enable us to believe that the spatio-temporal map of single point face video can calculate accurate blood pressure value.

Still, there are many challenges to indirect blood pressure measurements; the accuracy of blood pressure measurement is easily affected by many factors [5], including the professional abilities of the conductors, the height, weight, and age of the subjects, and the seasons and environments. For example, head motion creates difficulties for the region cutting algorithm, causes residual motion image, and degrades the image quality. In addition, the weak remote BVP signal reflecting changes in hemoglobin concentration in the circulatory system can easily be contaminated and submerged by changing ambient light. Moreover, because of difficulties of blood pressure data collection and the privacy issues

of face video, there is very few large-scale blood pressure database with face videos. The lack of data greatly hinders the rapid development in the field of non-contact measurement of blood pressure.

Therefore, this study is proposing the first end-to-end non-contact blood pressure measurement network based on face videos in this study. The main contributions are summarized as follows:

1. Proposes for the first time a non-contact end-to-end blood pressure measurement network named BPM-Net based on the face video.
2. Only a 15-second video sequence is needed to measure diastolic and systolic blood pressure, which has higher detection efficiency than traditional blood pressure measurement methods.
3. An oversampling training scheme for blood pressure monitoring task is proposed for the first time, which effectively addresses the uneven distribution of blood pressure data set in the training process.

2. Related work

Until now, two categories of methods have been used to measure blood pressure: direct and indirect measurements. Direct blood pressure measurements are made with medical equipment to directly monitor human biological signals [6, 7, 8, 9], including two main technical approaches. One route is to measure the pressure change directly with a pressure transducer, for example, arterial manometry [10]. The other technical approach is to control the pressure applied to the measured area by an external device and then use the information related to the Coriolis sound for blood pressure measurement. The most classic apparatus is the mercury sphygmomanometer [9], inexpensive and with high accuracy of measurement

Indirect blood pressure measurements usually calculate the systolic and diastolic blood pressure based on the features of measured BVP signals [11]. Pulse wave velocity (PWV) refers to the pressure wave velocity that propagates along

the wall of the great artery during each cardiac ejection. It is a simple, effective, and economic index for the noninvasive evaluation of arterial stiffness [12, 13]. Moreover, it is an independent predictor of cardiovascular events closely related to blood pressure [14, 15, 16, 17]. A series of simulation experiments on humans and animals confirmed that pulse wave transit time (PWT) is closely related to diastolic and systolic blood pressures. In this context, a novel indirect method, which differed from the traditional direct methods using cuff or oscilloscope devices, was proposed to measure blood pressure. In 2014 Rohan et al. introduced that the arterial blood pressure value can be calculated accurately based on the extracted features of BVP signals [18], which was obtained by the skin-contact noninvasive sensors derived from optical plethysmography (PPG) technology. After detecting the blood volume changes of the cardiac cycle with infrared light, the time delay of systolic and diastolic peak values was calculated to estimate the blood pressures. Another study added $1/2$ pulse width and $2/3$ pulse width as the characteristics of BVP signal together with systolic upstroke time and diastolic time [19]. However, in some previous studies, the relationship between blood pressure and BVP signals was assumed as nonlinear. Then, artificial neural networks were adopted to get more accurate models between the blood pressure and BVP signals [20, 21].

In order to obtain more characteristics related to blood pressure, some researchers [22] proposed that electrodes and instruments could collect ECG signals while PPG signals were obtained. At the same time, others designed a new sensor integrating PPG signal acquisition and ECG signal acquisition [23] and then eliminated baseline drift noise by wavelet change, which significantly improved the measured results. Similar to the development route of blood pressure detection method with only PPG, some papers [24] also used artificial neural network ANN to train the network model to predict blood pressure according to the sample experiment [24, 25]. Based on previous work, demographic information (including weight, height, and other factors) was added to the network for training. The results showed that the performance of the mode [26] obtained generated this way was much better than that of the multiple regression

method. In addition to the use of artificial neural networks and other network models, traditional machine learning method [13, 27, 28] was also used in many studies to optimize the feature extraction process. In 2021 Meng et al. showed that temporal and energy features of BVP signal obtained by face videos can also be adopted to estimate blood pressure comprehensively [26]

3. Methodology

This study proposes a non-contact blood pressure measurement network. There are five main steps in the proposed method, and the overall workflow is shown in Figure 1. Firstly, the ROI, which contains the blood pressure signal from the input facial video, needs to be defined. Secondly, the data augmentation (DA) module is proposed to cope with position drift and face motion artifacts in adjacent frames. Thirdly, in order to reduce interferences caused by illumination variations, the Color Space Conversion (CSC) module is proposed to transform RGB color space into YUVT color space. Then, to reduce interferences caused by sudden non-rigid motions, the ROI sequences are sliced to generate the multi-domain spatial-temporal mapping. Finally, the Blood Pressure Estimator module estimates systolic and diastolic blood pressure. Details of each module are explained in the following subsections.

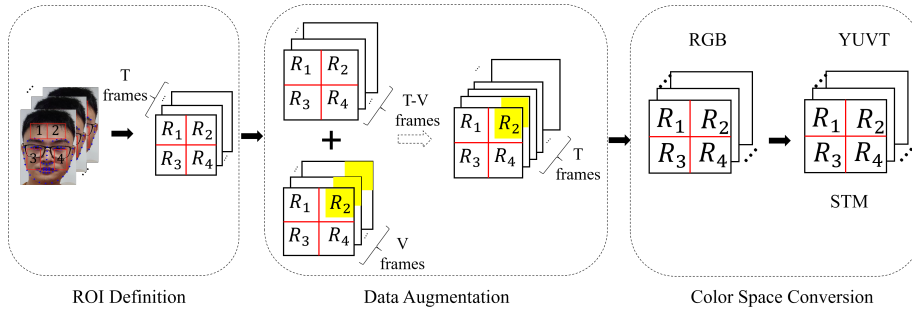


Figure 1: Overview of the module of ROI Definition and Data Augmentation. Seetaface6 is used to detect human face and localize 68 landmarks, which are then fed into the Data augmentation (DA) module and the color space conversion (CSC) module in turn

3.1. ROI Definition

In order to reduce the interference of background information and invalid face regions (such as eyes, nose, hair, and mouth), four regions of interest (ROIs) are defined by selecting the forehead and cheek with rich vascular information. First, the authors use SeetaFace6 to detect face and localize 68 landmarks and select 7 points to delineate the ROIs in each frame, as shown in Figure 1, total of N ROIs are selected. Next, we get the average pixel values of each ROI to represent physiological information. noted as:

$$f_{roi}(t, n) = R_n \quad (1)$$

where R_n represents four ROI regions at frame t as shown in Figure 2.

3.2. Data Augmentation

The change of external illumination easily interferes with the color information of the face video, which will affect the accuracy of non-contact blood pressure detection. Therefore, a data augmentation strategy is proposed to simulate the problem of signal contamination caused by external illumination changes thus improving the algorithm's robustness. First, the authors randomly select the segment with the length of V in the T frame sequence $f_{roi}(t, n), t \in V$, as shown in Figure 1. For selected frames, we randomly select a region, which is then masked and generate a new feature sequence $f'_{roi}(t, n), t \in V$.

The authors splice the frame sequences, $f'_{roi}(v, n), v \in V$ and $f_{roi}(t, n), t \notin V$ in the time dimension and form a new feature sequence recoded as $g'_{roi}(t, n), t \in T$. Finally, YUVT color space is proposed here to extract information related to BVP, which gives more attention to brightness dimension features in color space. The new color space transformation can be formulated as:

$$\begin{bmatrix} Y_t(x, y) \\ U_t(x, y) \\ V_t(x, y) \end{bmatrix} = \begin{bmatrix} 0.299 & 0.587 & 0.114 \\ -0.169 & -0.331 & 0.5 \\ 0.5 & -0.419 & -0.081 \end{bmatrix} \begin{bmatrix} R_t(x, y) \\ G_t(x, y) \\ B_t(x, y) \end{bmatrix} \quad (2)$$

where t indicates video frame index, $R_t(x, y), G_t(x, y), B_t(x, y) \in g'_{roi}(t, r_i)$, and $R_t(x, y), G_t(x, y), B_t(x, y)$ represents the pixel value in RGB color space, while $Y_t(x, y), U_t(x, y), V_t(x, y)$ are the pixel value of the YUVT color channel. All of them constitute the video sequence after data enhancement together. The enhanced video sequence is noted as spatial-temporal mapping (STM) $g_{roi}(t, n)$.

3.3. Architecture

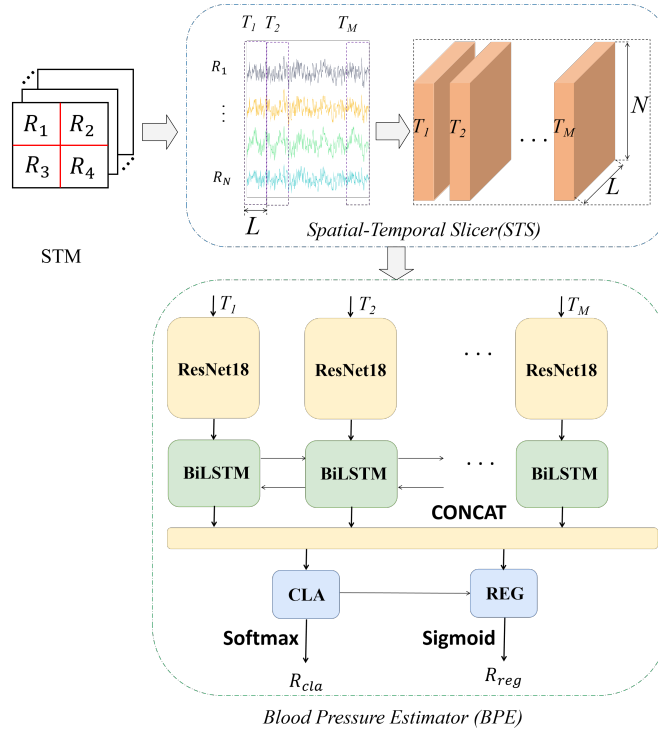


Figure 2: Architecture of the BPM-Net. Firstly, four ROIs are obtained by using detection points, and then each region is divided into N sub-ROIs. After all the sub-ROIs are expanded and sliced in time domain, M spatial-temporal feature maps $\{TS_1, TS_2, \dots, TS_M\}$ are generated.

3.3.1. Spatial-Temporal Slicer

For $g_{roi}(t, n)$, each subsets of ROI is pooled to get the average of each ROI pixel $AP(n, t)$, which can be stated as:

$$AP(n, t) = \frac{\sum_{x,y \in ROI_{i,n,t}} V(x, y, t)}{NUM} \quad (3)$$

Where $V(x,y,t)$ represents the pixel value of the n th subsets position (x, y) of frame t of the face video sequence, NUM represents the number of pixels in the selected ROI region. The average value of each subsets pixel is flattened and spliced to form the feature vector corresponding to the t frame, which can be written as :

$$SS(t) = CAT \left(\emptyset \left(\bigcup_{n=1}^N AP(n, t) \right) \right) \quad (4)$$

where \emptyset represents the extracting non empty subsets operation, and $CAT(\cdot)$ represents the feature vector splicing operation. We combine the eigenvectors of all frames into a spatial-temporal feature map, and divide them into two parts by sliding windows with step length L . M separate time-space fragments $\{T_1, T_2, \dots, T_M\}$ are constructed as multi-domain spatial-temporal feature mapping $STS(m)$, which can be defined as :

$$STS(m) = \bigcup_{t=N \times cl}^{(N+1) \times cl} SS(t) \quad (5)$$

where m is the index of spatial-temporal slicer. In order to use video information effectively and help network learning, I normalized the pixel values of all video frames to the range of $[0,1]$.

3.3.2. Blood Pressure Estimator

In this experiment, the residual convolution neural network [29] is used as the backbone network, and the size of all convolution kernels is 3×3 . The step is 1. Firstly, the feature extraction network module is used to perform high-dimensional feature extraction on the multi-temporal spatial feature map $STS(m)$. The feature extraction network corresponding to each time domain segment adopts the same parameters. The results are fed to the subsequent

LSTM to strengthen the temporal correlation and obtain the high-dimensional semantic features F . Then blood pressure classifier is used to classify the high-dimensional semantic features F to obtain the blood pressure interval. This operation can establish a benchmark for the features and effectively reduce the over fitting phenomenon of the network. Finally, The results of the classifier are integrated with the output of the feature extractor to calculate the specific value of blood pressure, which can also effectively help in classifier training.

We express the whole BPE process as the following formula:

$$F = \text{CAT} \left(\bigcup \text{FE}(\text{STS}(\text{m})) \right) \quad (6)$$

$$F_{\text{cla}} = \text{CLA}(F) \quad (7)$$

$$R_{\text{reg}} = \text{REG}(\text{CAT}(F, F_{\text{cla}})) \quad (8)$$

$$R_{\text{cla}} = \text{SOFTMAX}(F_{\text{cla}}) \quad (9)$$

where FE represents the feature extraction network composed of depth residual network and LSTM, $\text{CAT}(\cdot)$ represents dimension splicing operation, CLA represents blood pressure classifier, REG represents blood pressure calculator, R_{cla} represents the output features of classifier, R_{reg} represents the output results of classifier and calculator respectively, and $\text{SOFTMAX}(\cdot)$ represents softmax operation. We use the cross entropy loss function to train the classifier and MAE loss function to train the calculator. The two loss functions are combined to train the proposed model, which are formulated as follows:

$$\text{Loss}_{\text{cla}} = \frac{1}{N} \sum_i -[y_i \cdot \log(p_i) + (1 - y_i) \cdot \log(1 - p_i)] \quad (10)$$

$$\text{Loss}_{\text{reg}} = \frac{\sum_{i=1}^N |f_i - y_{fi}|}{N} \quad (11)$$

$$\text{Loss} = \text{Loss}_{\text{cla}} + \text{Loss}_{\text{reg}} \quad (12)$$

where p_i represents the result of classifier, f_i represents the result of calculator, y_i represents the category label of blood pressure truth value, y_{fi} represents the

truth value of blood pressure. The final output result needs to be calculated with the classifier result as the reference value and the deviation calibration of the calculator

$$R = \alpha \cdot STA(R_{cla}) + \beta \cdot R_{reg} \quad (13)$$

where STA represents the reference value of each blood pressure interval and the deviation weight, and α represents the weight of the calculator results, β represents the weight of the classifier results.

3.4. Oversampling training strategy

In order to deal with uneven distribution of data in different blood pressure intervals in datasets, an oversampling training strategy is proposed for the first time. First, according to the distribution and level of blood pressure, different grouping strategies are designed for systolic and diastolic pressure data, which is then divided into four big groups based on the value of blood pressure $\{G_1, G_2, G_3, G_4\}$. In the five-fold cross validation experiment, each big group was divided into five small groups equally again, four of them are as training set and the other one is as the validation set. For each batch, the ratio of samples from each large group is 1:1:1:1. Data is extracted from each group in order. If the quantity is insufficient, the sample will be selected from the beginning. The sampling strategy to construct training dataset group $ST(d, c)$ and validation dataset group $SV(d, c)$ can be respectively computed as:

$$ST(d, c) = \bigcup_{d=1}^4 (G_{dc}) \quad (14)$$

$$SV(d, c) = \bigcup_{d=1}^4 \left(\bigcup_{d=1}^c G_{dc} + \bigcup_{d=c+1}^5 G_{dc} \right) \quad (15)$$

where G_{dc} represents a small dataset group, and d and c indicates the times of cross-validation and the index of small group in each big group.

4. Experiments

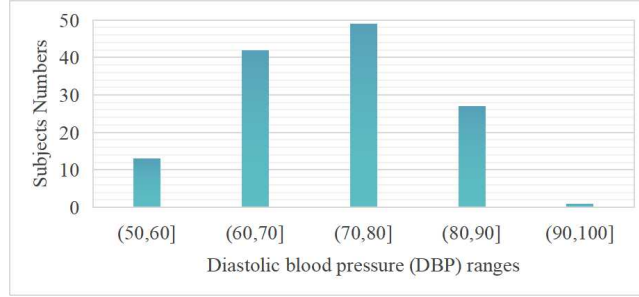
4.1. Dataset

The performance of the proposed network was evaluated on a public dataset and a private dataset. MMSE-HR [30] is a public non-contact heart rate and blood pressure estimation database composed of 102 face videos from 40 subjects and recorded at 25 frames per second (fps). A physiology data acquisition system was used to collect the average HR and BP values.

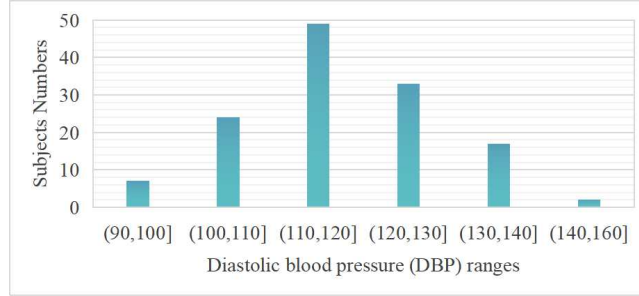
A private database for non-contact blood pressure estimation was created, named as Advanced Sensor Physiological Dataset (ASPD). In this dataset, the physiological data and corresponding face videos of 124 people were collected by using a multi-channel physiological signal acquisition system (Biopac M160), a blood pressure monitor (OMRON HEM-1020), and a mobile phone camera (Huawei Mate30), respectively. The face video for each subject was collected for about 1 minute. The frame rate of the video is 30fps, and the resolution is 1920×1080 . The distributions of systolic and diastolic blood pressures of ASPD dataset are shown in Figure 3. Moreover, the devices and setup is illuminated in Figure 4.

Three metrics were used to evaluate the performance of the network including the standard deviation (SD), the root mean square error (RMSE), and the mean absolute error (MAE).

In ASPD cross validation, all face videos were sampled to 30fps. Training was done with Nvidia-v100 and Pytorch. The authors designed independent oversampling learning strategy for systolic and diastolic blood pressure, and conducted independent cross validation and cross dataset testing. Firstly, a five-fold cross validation was performed on ASPD dataset, and comparative experiments were conducted to verify various key module parameters of the network and the optimal combination scheme. These parameters included the number of intercepted small ROIs, the type of loss function, the type and depth of backbone network, the color space, and the frame size. After that, ASPD was used to train and test cross datasets on MMSE-HR. Finally, a five-fold



(a)



(b)

Figure 3: The distributions of the ground-truth blood pressure values in ASPD dataset. (a) The systolic blood pressures. (b) The diastolic blood pressures.

cross-validation was performed on ASPD, and ablation experiments were done on the oversampling training scheme to verify its effectiveness.

4.2. Ablation study

4.2.1. The effectiveness of spatial-temporal slicer

In order to verify the effectiveness of the combination of the spatiotemporal slicer and LSTM, we use the oversampling training scheme to train systolic and diastolic blood pressure, respectively. The number of sub-ROIs in each ROI and the loss function used in training of SBP and DBP were set to 6, L1 and 4, L2 respectively. At the same time, they all used ResNet 50-512 as the backbone network and YUVT as the color space. It was predicted that the specific length of the spatiotemporal slicer would greatly affect the final training results, and

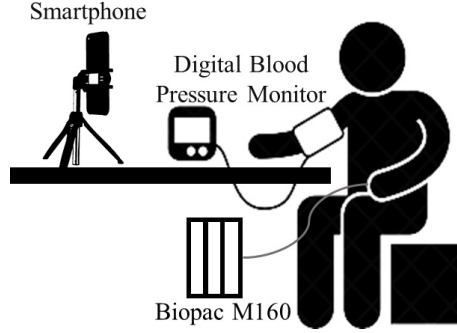


Figure 4: Devices and setup used in collecting ASPD.

the optimal scheme of spatiotemporal slicing could be found. Clip length was tested for 90,150,225 and 450.

From Table 1, spatiotemporal slicer with LSTM can help the network obtain the detailed characteristics of physiological information more effectively, and the slice length of 150 frames can maximize the effect of this network combination. For example, as shown in Table 1, MAE of systolic blood pressure and diastolic blood pressure reached 8.07mmHg and 6.78mmHg, respectively. Compared with other slice length schemes, MAE of systolic blood pressure and diastolic blood pressure increased by 0.37mmHg and 0.55mmHg, respectively, which was much better than the network scheme without temporal and spatial slices (15.78 mmHg and 15.04 mmHg, respectively). Then observe SD and RMSE. In practical measurement, the number of observations n is always limited, and the actual value can only be replaced by the most reliable (optimal) value. RMSE is susceptible to a group of significant or minor errors in measurement, so it can well reflect measurement precision. It can be seen from the table that RMSE and SD of the 150 slice length scheme are still the best, which shows that this scheme not only improves accuracy but also enhances stability.

4.2.2. The effectiveness of oversampling strategy(OSS)

Then the effectiveness of the oversampling training scheme was tested, with the standard data sampling training scheme as a comparison (in each epoch,

Table 1: Performance comparison of different network.

	Method	SD(mmHg)	RMSE (mmHg)	MAE(mmHg)
SBP	Without LSTM	10.49	17.85	15.78
	LSTM-90	10.06	10.33	8.44
	LSTM-150	9.81	9.94	8.07
	LSTM-225	10.09	10.16	8.32
DBP	Without LSTM	9.28	17.06	15.04
	LSTM-90	8.35	9.12	7.31
	LSTM-150	8.28	8.45	6.78
	LSTM-225	8.33	9.05	7.33

Notes: Red indicates the best performance of different network.

Table 2: Performance comparison of different networks.

	Method	SD(mmHg)	RMSE (mmHg)	MAE(mmHg)
SBP	With OSS	9.81	9.94	8.07
	Without OSS	10.12	10.14	8.27
DBP	With OSS	8.28	8.45	6.78
	Without OSS	8.35	8.6	6.92

Notes: Red indicates the best performance of different training strategy.

training samples were imported into the network for training). The above results show that the combination of spatiotemporal slice and LSTM is the best when clip length is 150. Therefore, in this test, LSTM-150 was used as the primary network structure. Table 2 shows that the training scheme enabled the same network model with more vital fitting ability and robustness. MAE of systolic blood pressure and diastolic blood pressure decreased from 8.27mmHg and 6.92mmHg to 8.07mmHg and 6.78mmHg. RMSE also decreased by 0.2mmHg and 0.15mmHg, respectively. This shows that for the blood pressure task with

few training samples, appropriate oversampling training scheme is helpful to further enhance the network potential.

4.3. Cross-dataset testing

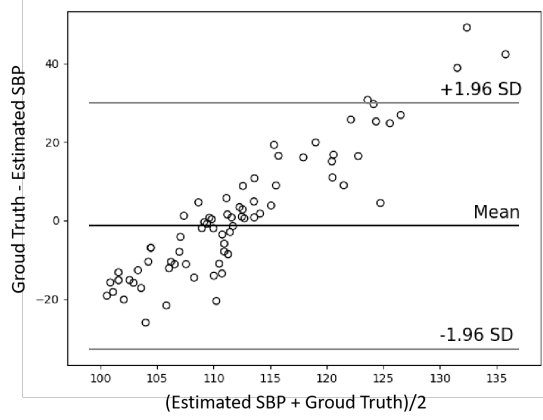
Table 3: Results of BP measurements

	Method	SD(mmHg)	RMSE (mmHg)	MAE(mmHg)
SBP	NIBPP [31]	—	—	13.6
	NCBP [26]	19.81	22.43	17.52
	LSTM-90	17.02	17.35	13.42
	LSTM-150	16.02	16.55	12.35
	LSTM-225	16.98	17.12	13.15
DBP	NIBPP [31]	—	—	10.3
	NCBP [26]	15.21	15.23	12.13
	LSTM-90	13.34	13.44	10.41
	LSTM-150	11.98	12.22	9.54
	LSTM-225	12.87	13.22	10.33

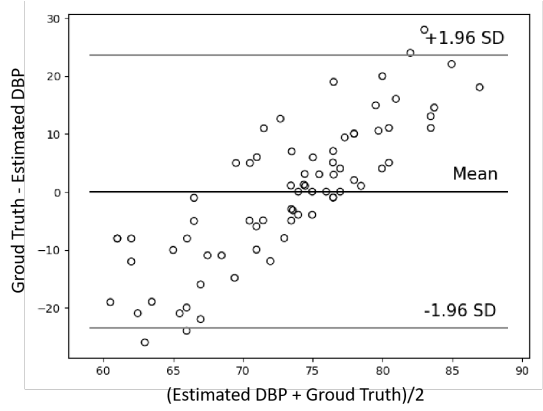
Notes: Red indicates the best performance of different methods.

A recent study provide a solution for blood pressure estimation based on rPPG. It used thousands of data for training, and 50 samples for test [31]. For our BPM-Net, 125 data samples are used for training and MMSE-HR data are used for testing. The sample ratio tends to be close to 1:1. After three fine-tuning of the model, our BPM-Net obtained the best performance for the test is that the systolic blood pressure MAE is 13.6mmHg and the diastolic blood pressure MAE is 10.3mmHg. The comparative results are shown in Table3, We reproduced the NCBP [26] algorithm, trained it with ASPD and tested it on MMSE-HR. Besides the results of NIBPP [31] on its test data set (about 20 people) are also placed in the table for comparison From the results, it can be seen that, our method get better performance than the recent study. In order

to verify the effectiveness of BPM-Net, the Bland-Altman plots as showed in Figure 5 show a good consistency between the estimated blood pressure and the ground truth.



(a)



(b)

Figure 5: The Bland-Altman plots of the estimated (a) systolic blood pressure and (b) diastolic blood pressures comparing with their ground truths.

5. Conclusion

This paper presents the first non-contact end-to-end blood pressure measurement network, which only uses face video information to quickly calculate

diastolic and systolic blood pressure in 15 seconds. Tests have been run on the public dataset MMSE-HR and the self-collected data set ASPD, and the results show that the proposed BPM-Net can effectively and efficiently measure blood pressure.

Acknowledgments

This work is supported by the Sichuan Science and Technology Program under Grant 2022YFS0032 to Xiujuan Zheng, the Shaanxi Provincial Natural Science Basic Research Program under Grant 2021JQ-455 to Bin Li. The authors would like to thank the engineers of Xi'an Singularity Fusion Information Technology Co. Ltd for their supports of data collection and experimental procedures.

Declaration of competing interest

The authors declare that they have no known competing financial interests or personal relationships that could have appeared to influence the work reported in this paper.

References

- [1] D. Barvik, M. Cerny, M. Penhaker, N. Noury, Noninvasive continuous blood pressure estimation from pulse transit time: A review of the calibration models, *IEEE Reviews in Biomedical Engineering* 15 (2022) 138–151. doi:10.1109/RBME.2021.3109643.
- [2] A. Chandrasekhar, M. Yavarimanesh, K. Natarajan, J.-O. Hahn, R. Mukkamala, Ppg sensor contact pressure should be taken into account for cuff-less blood pressure measurement, *IEEE Transactions on Biomedical Engineering* 67 (11) (2020) 3134–3140. doi:10.1109/TBME.2020.2976989.

- [3] X. Niu, S. Shan, H. Han, X. Chen, Rhythmnet: End-to-end heart rate estimation from face via spatial-temporal representation, *IEEE Transactions on Image Processing* 29 (2020) 2409–2423. doi:10.1109/TIP.2019.2947204.
- [4] J. Cheng, Y. Xu, R. Song, Y. Liu, C. Li, X. Chen, Prediction of arterial blood pressure waveforms from photoplethysmogram signals via fully convolutional neural networks, *Computers in Biology and Medicine* 138 (2021) 104877. doi:10.1016/j.compbiomed.2021.104877.
- [5] N. Markandu, F. D. Witcher, A. Arnold, C. Carney, The mercury sphygmomanometer should be abandoned before it is proscribed, *Journal of Human Hypertension* 14 (2000) 31–36. doi:10.1038/sj.jhh.1000932.
- [6] G. L. Young P, A surrogate arm for evaluating the accuracy of instruments for indirect measurement of blood pressure, *Biomed Instrum Technol* 24 (1990) 130–135.
- [7] K. Kario, Home blood pressure monitoring: Current status and new developments, *Am J Hypertens* 34 (2021) 783–794.
- [8] M. A. Ulrich Tholl, Klaus Forstner, Measuring blood pressure: pitfalls and recommendations, *Nephrol Dial Transplant* 19 (2004) 766–70. doi:10.1093/ndt/gfg602.
- [9] G. Beevers, G. Lip, E. O’Brien, Abc of hypertension: Blood pressure measurement. part ii-conventional sphygmomanometry: technique of auscultatory blood pressure measurement, *BMJ (Clinical research ed.)* 322 (2001) 1043–7.
- [10] G. L. Pressman, P. M. Newgard, A transducer for the continuous external measurement of arterial blood pressure, *IEEE Transactions on Bio-medical Electronics* 10 (2) (1963) 73–81. doi:10.1109/TBMEL.1963.4322794.
- [11] T. Knight, F. Leech, A. Jones, L. Walker, R. Wickramasinghe, S. Angris, P. Rolfe, Sphygmomanometers in use in general practice:an overlooked as-

- pect of quality in patient care, *Journal of Human Hypertension* 15 (2001) 681–684. doi:10.1038/sj.jhh.1001251.
- [12] B. Gribbin, A. Steptoe, P. Sleight, Pulse wave velocity as a measure of blood pressure change, *Psychophysiology* 13 (1976) 86–90.
 - [13] S. S. Mousavi, M. Firouzmand, M. Charmi, M. Hemmati, M. Moghadam, Y. Ghorbani, Blood pressure estimation from appropriate and inappropriate ppg signals using a whole-based method, *Biomedical Signal Processing and Control* 47 (2019) 196–206. doi:10.1016/j.bspc.2018.08.022.
 - [14] M. Landowne, A method using induced waves to study pressure propagation in human arteries, *Circulation Research* 5 (1957) 594–601.
 - [15] R. A. Payne, C. N. Symeonides, D. J. Webb, S. R. J. Maxwell, Pulse transit time measured from the ecg: An unreliable marker of beat-to-beat blood pressure, *Journal of Applied Physiology* 100 (2006) 136–141. doi:10.1152/jappphysiol.00657.2005.
 - [16] L. A. Geddes, M. H. Voelz, C. F. Babbs, J. D. Bourland, W. A. Tacker, Pulse transit time as an indicator of arterial blood pressure, *Psychophysiology* 18 (1) 71–74. doi:10.1111/j.1469-8986.1981.tb01545.x.
 - [17] X. Fan, Q. Ye, X. Yang, S. Choudhury, Robust blood pressure estimation using an rgb camera, *Journal of Ambient Intelligence and Humanized Computing* 11. doi:10.1007/s12652-018-1026-6.
 - [18] R. Samria, R. Jain, A. Jha, S. Saini, S. R. Chowdhury, Noninvasive cuffless estimation of blood pressure using photoplethysmography without electrocardiograph measurement, in: 2014 IEEE REGION 10 SYMPOSIUM, 2014, pp. 254–257. doi:10.1109/TENCONSpring.2014.6863037.
 - [19] X. Teng, Y. Zhang, Continuous and noninvasive estimation of arterial blood pressure using a photoplethysmographic approach, in: Proceedings of the 25th Annual International Conference of the IEEE Engineering in Medicine

- and Biology Society (IEEE Cat. No.03CH37439), Vol. 4, 2003, pp. 3153–3156 Vol.4. doi:10.1109/IEMBS.2003.1280811.
- [20] Y. Kurylyak, F. Lamonaca, D. Grimaldi, A neural network-based method for continuous blood pressure estimation from a ppg signal, in: 2013 IEEE International Instrumentation and Measurement Technology Conference (I2MTC), 2013, pp. 280–283. doi:10.1109/I2MTC.2013.6555424.
 - [21] L. Wang, W. Zhou, Y. Xing, X. Zhou, A novel neural network model for blood pressure estimation using photoplethysmography without electrocardiogram (2018) 1–9doi:10.1155/2018/7804243.
 - [22] Z. Shen, F. Miao, Q. Meng, Y. Li, Cuffless and continuous blood pressure estimation based on multiple regression analysis, in: 2015 5th International Conference on Information Science and Technology (ICIST), 2015, pp. 117–120. doi:10.1109/ICIST.2015.7288952.
 - [23] D. Han, J. Zhang, S. Shan, Leveraging auxiliary tasks for height and weight estimation by multi task learning, in: 2020 IEEE International Joint Conference on Biometrics (IJCB), 2020, pp. 1–7. doi:10.1109/IJCB48548.2020.9304855.
 - [24] J. Y. Kim, B. H. Cho, S. M. Im, M. J. Jeon, I. Y. Kim, S. Kim, Comparative study on artificial neural network with multiple regressions for continuous estimation of blood pressure, in: 2005 IEEE Engineering in Medicine and Biology 27th Annual Conference, 2005, pp. 6942–6945. doi:10.1109/IEMBS.2005.1616102.
 - [25] N. Maher, G. Elsheikh, W. Anis, T. Emara, Non-invasive Calibration-Free Blood Pressure Estimation Based on Artificial Neural Network, 2020, pp. 701–711. doi:10.1007/978-3-030-14118-9_69.
 - [26] M. Rong, K. Li, A blood pressure prediction method based on imaging photoplethysmography in combination with machine learning, Biomedical

- Signal Processing and Control 64 (2021) 102328. doi:10.1016/j.bspc.2020.102328.
- [27] R. He, Z.-P. Huang, L.-Y. Ji, J.-K. Wu, H. Li, Z.-Q. Zhang, Beat-to-beat ambulatory blood pressure estimation based on random forest, in: 2016 IEEE 13th International Conference on Wearable and Implantable Body Sensor Networks (BSN), 2016, pp. 194–198. doi:10.1109/BSN.2016.7516258.
 - [28] Y. Zhang, Z. Feng, A svm method for continuous blood pressure estimation from a ppg signal, Proceedings of the 9th International Conference on Machine Learning and Computing.
 - [29] Z. Yu, X. Li, G. Zhao, Remote photoplethysmograph signal measurement from facial videos using spatio-temporal networks, in: 30th British Machine Vision Conference 2019, BMVC 2019, Cardiff, UK, September 9-12, 2019, BMVA Press, 2019, p. 277.
 - [30] S. Tulyakov, X. Alameda-Pineda, E. Ricci, L. Yin, J. F. Cohn, N. Sebe, Self-adaptive matrix completion for heart rate estimation from face videos under realistic conditions, in: 2016 IEEE Conference on Computer Vision and Pattern Recognition (CVPR), 2016, pp. 2396–2404. doi:10.1109/CVPR.2016.263.
 - [31] F. Schrumpf, P. Frenzel, C. Aust, G. Osterhoff, M. Fuchs, Assessment of non-invasive blood pressure prediction from ppg and rppg signals using deep learning, Sensors 21 (18). doi:10.3390/s21186022.